JACS
JOURNAL OF THE AMERICAN CHEMICAL SOCIETY
Article
pubs.acs.org/JACS

Nature of Valence Transition and Spin Moment in Ag_nV^+ Clusters

Victor M. Medel,[†] Arthur C. Reber,[†] Vikas Chauhan,[‡] Prasenjit Sen,[‡] Andreas M. Köster,*[,§] Patrizia Calaminici,*[,§] and Shiv N. Khanna*[,†]

[†]Department of Physics, Virginia Commonwealth University, Richmond, Virginia 23284-2000, United States
[‡]Harish-Chandra Research Institute, Chhatnag Road Jhunsi, Allahabad 211019, India
[§]Departamento de Química, Cinvestav, Avenida Instituto Politécnico Nacional 2508 A.P. 14-740, Ciudad de México 07000, México

Supporting Information

ABSTRACT: Evolution in the atomic structure, bonding characteristics, stability, and the spin magnetic moment of neutral and cationic Ag_nV clusters has been investigated using first-principles density functional approach with gradient corrected functional. It is shown that at small sizes, the V 4s states hybridize with Ag states to form 1S and 1P like superatomic orbitals, whereas the 3d states are localized on V giving the V atom an effective valence of 1 or 2. Starting from Ag_8V^+, the V 3d states begin to participate in the bonding by hybridizing with the nearly free electron gas to form 1D superatomic orbitals increasing the V atom effective valence toward 5. For the cationic clusters, this changing valence results in three shell closures that lead to stable species. These occur for cationic clusters containing 5, 7, and 14 Ag atoms. The first two stable species correspond to filled 1S and 1P shells in two and three dimensions with a valence of 2 for V, whereas the closure at 14 Ag atoms correspond to filled 1S, 1P, and 1D shells with V site exhibiting a valence of 5. The transition from filled 1S and 1P shells to filled 1S, 1P, and 1D shells is confirmed by a quenching of the spin magnetic moment. The theoretical findings are consistent with the observed drops in intensity in the mass spectrum of Ag_nV^+ clusters after 5, 7, and 14 Ag atoms.

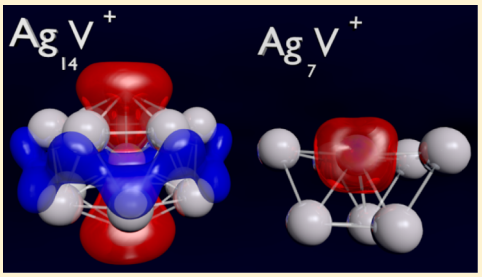

An atom's effective chemical valence, the number of electrons that are involved in forming chemical bonds is a fundamental concept for understanding the behavior of an atom. Depending on the atom's identity and environment, a particular element can exhibit multiple valences. Typically, simple metals such as alkali metals are monovalent and alkaline earth elements are divalent, whereas transition elements can exhibit multiple valence. Consider the case of a V atom with an electronic configuration of [Ar] $3d^3$ $4s^2$. It may exhibit a valence of 2 if only the $4s^2$ electrons are involved in the bonding or 5 if both the $4s^2$ and $3d^3$ electrons hybridize with neighboring species to form molecular orbitals. Another possibility exists if the first excited state of the V atom with the electronic configuration [Ar] $3d^4$ $4s^1$ is involved in the bonding. By bonding only via the 4s electron, even monovalent V can be found. In this study, we investigate how the orbitals of the nearly free electron gas in silver effect the valence of V in $Ag_nV^{0/+}$ clusters. We will demonstrate that the valence of V oscillates between 1 or 2 at small cluster sizes and transitions to 5 as the number of Ag atoms is increased and that this valence transition explains the changes in stability and magnetic moment of $Ag_nV^{0/+}$ clusters.

The electronic states in small symmetric metal clusters are bunched into shells.[1−6] This was pointed out by Knight and co-workers in an observation of the mass spectra of small sodium clusters.[1] They proposed that a simple jellium model, where the positive charge of all the ions in the cluster is distributed uniformly over a sphere of the size of the cluster, that resulted in a grouping of the energy levels into shells that can be labeled by principal and angular momentum quantum numbers much in the same way as in atoms: 1S, 1P, 1D, 2S, 1F, 2P...[7−11] The nearly free electron gas models account for observed variations in the polarizability, ionization energy, and electron affinity in metal clusters,[1,12−14] and experiments have demonstrated that clusters with filled shells exhibit chemical inertness.[15−22] These findings form the conceptual basis for regarding stable clusters as superatoms.[23−30] For pure silver clusters, the structure, stability, and electronic properties can be rationalized on the basis of such a confined nearly free electron picture with each silver atom donating one delocalized 5s electron.[31−38] Clusters such as Ag_{15}^+, Ag_{14}, and Ag_{13}^- contain 14 valence electrons that do not correspond to a filled shell in a spherical jellium; however, the clusters undergo geometrical distortions that lead to crystal field like splitting of the 1D orbital forming highly stable species.[38−43] The properties of pure silver clusters can be understood through a nearly free electron gas, so how do these delocalized orbitals effect the valence of transition metal atoms embedded in the cluster?[44−51]

Our studies are motivated by the work of Janssens et al.[52,53] who have carried out experimental studies on the stability of Ag_nV^+ clusters by forming the clusters in beam and then fragmenting them through irradiation. The mass spectra of the resulting species should be an indicative of the stability of the

Received: November 26, 2013
Published: May 13, 2014

 © 2014 American Chemical Society dx.doi.org/10.1021/ja412064c | J. Am. Chem. Soc. 2014, 136, 8229−8236

clusters. For Ag_nV^+ clusters, their mass spectra show three features. A small drop in intensity after Ag_5V^+ with more marked drop in intensity after Ag_7V^+ and after $Ag_{14}V^+$. Janssens et al. propose that V has a valence of 2 for Ag_7V^+, giving it 8 valence electrons and a valence of 5 at $Ag_{14}V^+$ to give it 18 valence electrons. This valence assignment grants the stable clusters magic numbers. Detailed theoretical investigations are needed to understand the microscopic mechanism, which explains the drop in intensity after Ag_5V^+, Ag_7V^+, and after $Ag_{14}V^+$, and to understand how the V 3d electrons participate in bonding.

The main objective of the present paper is to critically analyze the evolution of the electronic structure of neutral and cationic Ag_nV clusters containing up to 15 Ag atoms to answer some of the above questions. The key issues we want to address are as follows. (1) What is the valence of V at small sizes? Do the V 3d states participate in bonding or the V atoms maintain 3 unpaired d electrons at small sizes? (2) How does the valence and the magnetic moment of V change as successive Ag atoms are added to make larger species? (3) Is the valence change monotonic or the valence can fluctuate with size? (4) How does the spin magnetic moment get quenched as successive Ag atoms are added? (5) Are there $Ag_nV^{0/+}$ clusters whose stability is governed by geometric shell closures as in the case of several metal clusters including calcium and magnesium[54,55]

THEORETICAL METHODS

Studies of the electronic structure of Ag_nV clusters were carried out using a first-principles density functional (DFT) approach where the exchange correlation effects are included within a generalized gradient corrected (GGA) functional proposed by Perdew and Wang (PW86).[56,57] The electronic states of the cluster are expressed in a linear combination of Gaussian-type orbitals centered at the atomic sites. The deMon2k software[58−61] was used where a variational fitting of the Coulomb potential is employed to avoid the calculation of four-center electron repulsion integrals.[60] Also, the exchange−correlation potential and energy is calculated via the numerical integration of the Kohn−Sham density. A default adaptive grid of deMon2k with a grid accuracy of 10^{-5} a.u. was used.[62] A GGA optimized DZVP basis set[59] was used for the V atom that ensures, in combination with the PW86 functional, the correct ordering of the atomic V and V^+ states.[62] For Ag, a quasirelativistic effective core potential[63] with 19 valence electrons and the corresponding valence basis set was employed. To further reduce the computational effort, the auxiliary density was expanded in primitive Hermite Gaussian functions using the GEN-A2 auxiliary functional set.[59] The ground state atomic configurations were determined by starting from several initial configurations with various multiplicities and by optimizing without constrains in delocalized internal coordinates.[61] In order to explore as extensively as possible the potential energy surfaces (PESs) of the studied clusters and to look for any additional structure to be included in the search for the ground state, we performed canonical Born−Oppenheimer molecular dynamics (BOMD) simulations at 700 K for each cluster size. The BOMD simulations were run for up to 20 ps and starting from the obtained minima structures. The temperature was controlled by a Nosé−Hoover chain thermostat, and a step size of 2 fs was used. At every 200 fs of the BOMD trajectories, initial structures for local optimizations without including any symmetry restriction were taken. Therefore, for each cluster size, one hundred local optimizations have been performed. A frequency analysis was carried out to ensure the stability of the ground states. The lowest harmonic frequencies are listed in Table SI-V of the Supporting Information. For the Bader population analyses,[64,65] all-electron GGA optimized DZVP basis sets are used for all atoms in the clusters. As the present study also relates to the valence of the V site, we also investigated the electronic ground states of V and V^+ in different electronic configurations. The results are included in Table SI-I in the Supporting Information, where the calculated values are compared with available experimental values.

RESULTS

Figure 1 shows the atomic structures and spin multiplicities of the $Ag_nV^{0/+}$ ($4 \le n \le 15$) clusters. In the case of Ag_6V^+,

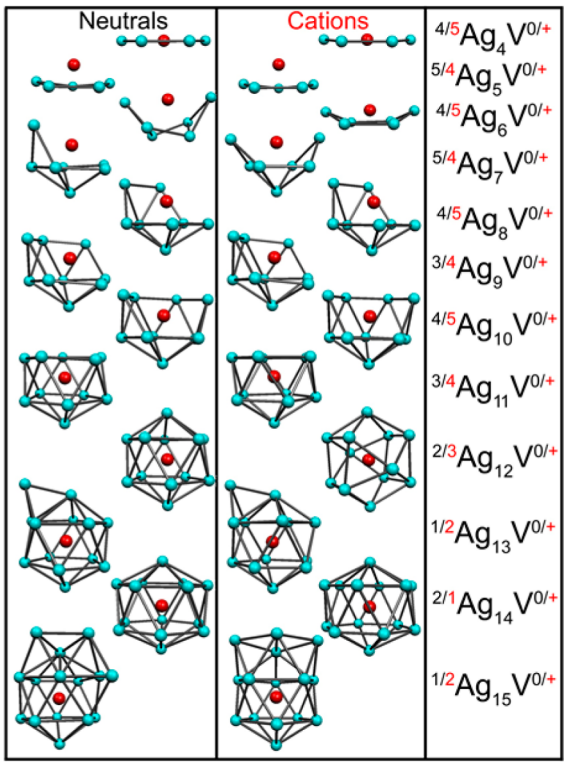

Figure 1. Ground state structures of $Ag_nV^{0/+}$ clusters and their spin multiplicities for $4 \le n \le 15$. The cyan and red spheres correspond to Ag and V atoms, respectively.

$Ag_{10}V^{0/+}$, and $Ag_{15}V^0$ clusters, we also found isoenergetic structures to the reported ground states. The Cartesian coordinates of all these minima structures are given in the Tables SI-II and SI-III of the Supporting Information. For either neutral or cationic structures in the first two cluster sizes (n = 4 and 5), the Ag atoms form planar structures. As the number of Ag atoms increases, the silver framework becomes three-dimensional. This progression in geometry is similar to the case of pure silver clusters, which become nonplanar at Ag_7, and as in alkali and copper clusters.[66−69] The case of $^5Ag_6V^+$ is particularly interesting as it has a quasiplanar structure, with 4 Ag atoms forming a square plane and the V atom above the center of that square. The remaining two Ag atoms are above the opposite edges of the square and aligned with the V atom. From n = 7 through n = 12, any additional Ag atom is just one more vertex in the icosahedra, and the V atom is gradually

dx.doi.org/10.1021/ja412064c | J. Am. Chem. Soc. 2014, 136, 8229−8236

encapsulated in the center by the Ag atoms for all the cases in $Ag_nV^{0/+}$ except for $^3Ag_{12}V^+$, which is a cuboctahedron. Actually, the $^{2/3}Ag_{12}V^{0/+}$ is the smallest cluster where the V is totally encapsulated, and as we will show, it is highly stable. The $^{1/2}Ag_{13}V^{0/+}$ structures are just the icosahedron with one Ag atom decorating one of the triangular faces. The addition of one more Ag atom results in the gyroenlongated hexagonal bipyramidal structure for $^{2/1}Ag_{14}V^{0/+}$, in which structure the 14 silver atoms completely encapsulates the V atom. The structures of $^{1/2}Ag_{15}V^{0/+}$ are just the icosahedron with three more Ag atoms decorating the triangular faces of it. The $^1Ag_{13}V$ and $^1Ag_{14}V^+$ are the first clusters with a completely quenched magnetic moment. We are particularly interested in the Ag_5V^+, Ag_7V^+, and $Ag_{14}V^+$ clusters as the experiments show a drop in intensity after these sizes.

Figure 2 shows the average distances of Ag−Ag and Ag−V for neutral and cationic clusters. The Ag−Ag average distance

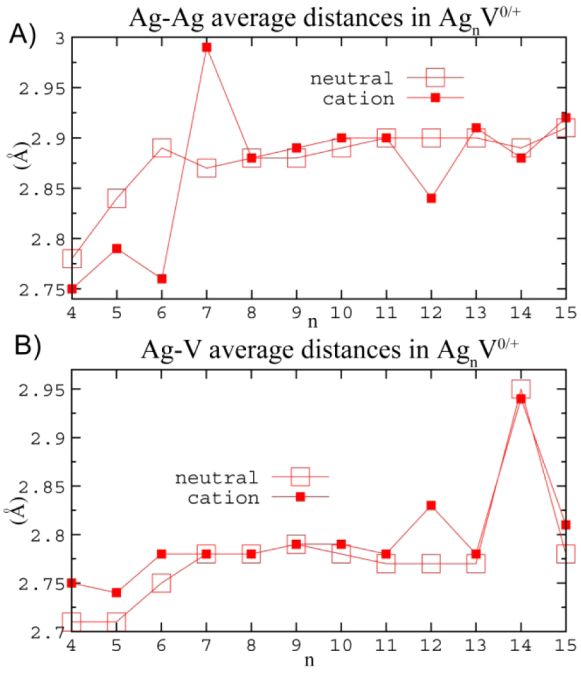

Figure 2. Average atom distances (in angstroms) in $Ag_nV^{0/+}$ clusters. In (A) the Ag−Ag and in (B) the Ag−V distances. The empty box symbol is for the neutral, and the filled box is for the cationic clusters.

for the neutrals tends to increase with the size, where there is a small local maxima at n = 6 and a shallow local minima at n = 14, which indicates an expansion or contraction of the cage, respectively. For the cations, we observe an initial alternation of the Ag−Ag average distance with maxima for Ag_5V^+ and Ag_7V^+. The pronounced maximum for Ag_7V^+ arises from an opening of the structure compared to its neutral counterpart. The other obvious feature in the Ag−Ag average distance is the local minimum for $Ag_{12}V^+$ that coincides with a local maximum for the Ag−V average distance in this cluster. This feature is caused by the very high symmetry cuboctahedral (O_h) geometry of the $Ag_{12}V^+$ cluster that may be thought of as having a closed geometric shell. The $Ag_{12}V^+$ cage has Ag−Ag bonds that are 2.84 Å. In contrast, the icosahedral Ag cage of the neutral $Ag_{12}V$ is considerably deformed with the Ag−Ag bond lengths varying between 2.85 and 3.08 Å.

Besides the already discussed maximum for $Ag_{12}V^+$ in the Ag−V average distance, other pronounced maxima appear for the neutral and cationic $Ag_{14}V$ clusters. They originate from the geometrical structure of these clusters. Because the Ag atoms form a doubly capped hexagonal antiprism, their distances to the central V atom vary between 2.65 Å for the two capping atoms and ∼3 Å for the 12 Ag atoms in the antiprism. In general, the Ag−V average distance is smaller than the corresponding Ag−Ag distance. A notable exception is the $^3Ag_{12}V^+$ cuboctahedron, in which the Ag−Ag and Ag−V distances are equal due to symmetry.

The main focus of the current work is to investigate the nature of bonding between the V and Ag atomic orbitals in order to identify the valence state of the V. To this end, we examined the nature of electronic states in the cationic clusters. Figures 3−5 present the electronic states and the associated

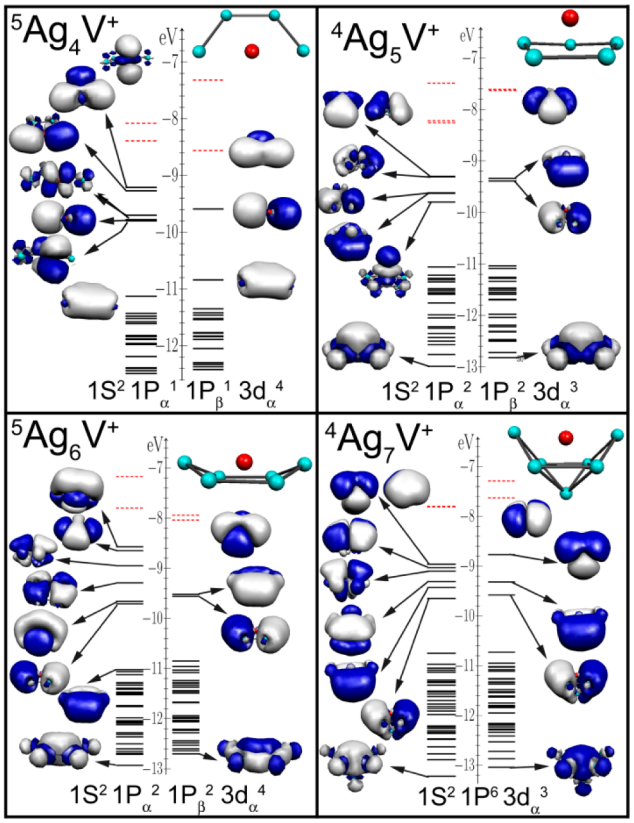

Figure 3. One-electron energy levels and molecular orbital wave function isosurfaces (isoval = 0.01 au) of Ag_nV^+ ($4 \le n \le 7$).

electronic orbitals corresponding to majority and minority states in the valence region of the clusters. For clarity, the electronic orbitals corresponding to 4d atomic states of silver atoms, which correspond to a dense band of states, are not marked. Further, the valence electronic states have been assigned an orbital character based on their effective quantum numbers (1S, 1P, 3d, 2S) through the examination of the nodes in the corresponding molecular orbitals. The continuous lines correspond to filled while the dotted lines represent unfilled states.

We first examine $^5Ag_4V^+$ in Figure 3, which has a planar configuration with a spin multiplicity of 5 that is larger than that of the ^4V atom. The majority spin and minority spin channel both have filled 1S, and $1P_x$ like orbitals. The $1P_y$ state is higher

dx.doi.org/10.1021/ja412064c | J. Am. Chem. Soc. 2014, 136, 8229−8236

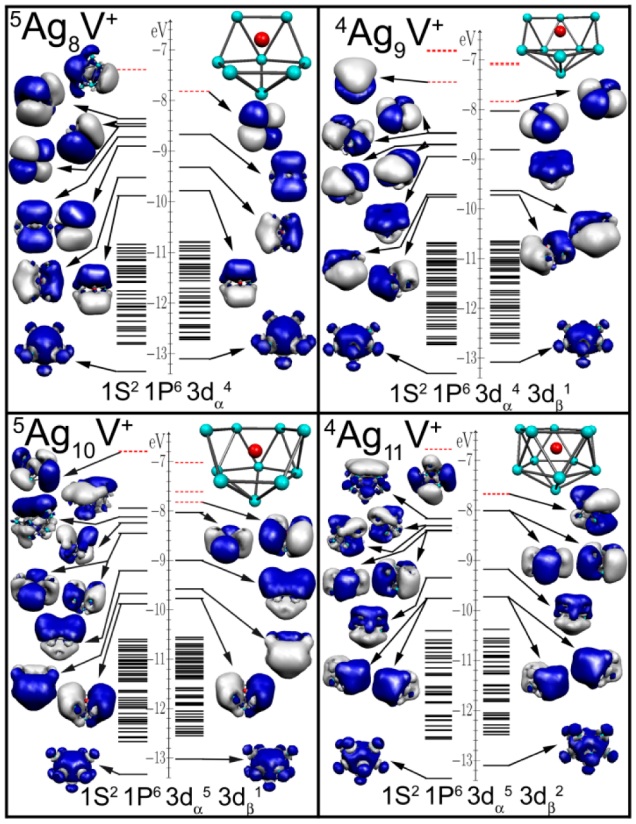

Figure 4. One-electron energy levels and molecular orbital wave function isosurfaces (isoval = 0.01 au) of Ag_nV^+ ($8 \le n \le 11$).

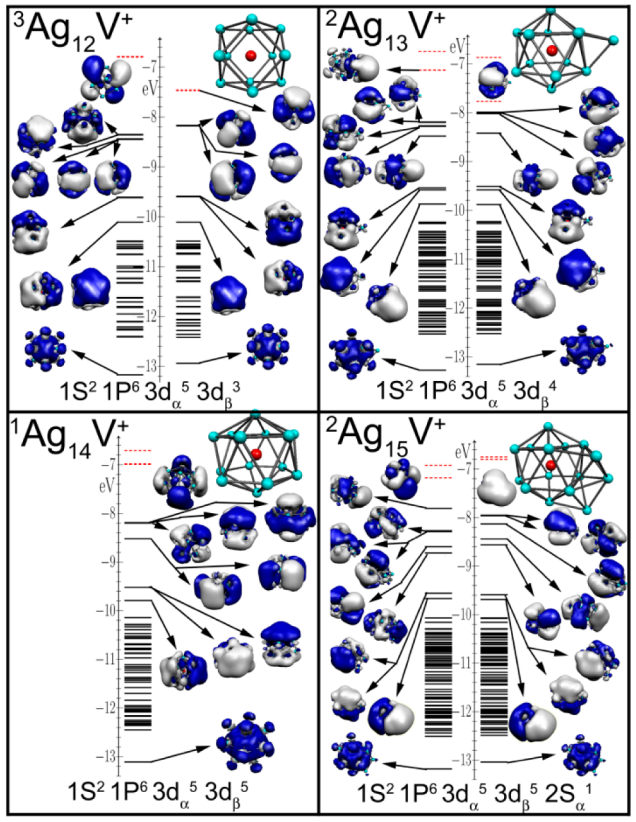

Figure 5. One-electron energy levels and molecular orbital wave function isosurfaces (isoval = 0.01 au) of Ag_nV^+ ($12 \le n \le 15$).

in energy resulting in the occupation of four 3d-like orbitals, the origin of the increased multiplicity. This indicates that at this small size, the V atom has an effective configuration of $4s^13d^4$ and as the V atom has effectively donated one valence electron to the delocalized 1S and 1P shells. There are four 3d electrons localized on the V atom and V contributes one electron that hybridizes with the nearly free electron gas. The $^4Ag_5V^+$ has filled 1S, $1P_x$, and $1P_y$ orbitals for both spin channels and three electrons in the majority V 3d states, indicating an effective valence of 2 for V. In the case of $^5Ag_6V^+$, the Ag atoms form a structure that is slightly deformed from a planar structure. The cluster has filled 1S, $1P_x$, and $1P_y$ orbitals in both spin channels, and the remaining four majority electrons occupy states with 3d-character, two of which are in the *xy* plane, whereas the other two with lobes perpendicular. Note that the almost planar structure by Ag atoms does not favor the formation of $1P_z$-like orbitals, so six electrons fill the 1S and 1P orbitals, leaving four electrons to fill 3d orbitals with meaningful exchange splitting. This indicates that V has a valence of 1.

$^4Ag_7V^+$ has a less planar structure than the previously considered clusters. The sequence of filled orbitals now corresponds to 1S, $1P_x$, $1P_y$, $1P_z$, filled orbitals in both spin channels and three electrons in 3d-like orbitals spread over the cluster. The filled $1S^2$ $1P^6$ shells with eight valence electrons correspond to a magic number in the confined free electron gas and, as we will show, the cluster exhibits enhanced stability. Also note that because the V 3d states do not participate in bonding, the V atom can be regarded as having a valence of 2. We note that the highest occupied molecular orbital (HOMO) in the spin up channel is 48% constructed from V 3d orbitals and 52% from Ag 5s orbitals. In the case of a spherical silver cluster with a V atom at the center, the idealized molecular orbital scheme is a $1S^2$ orbital followed by $1P^6$, and then the $1D^{10}$, as is the case with a nearly free electron gas; however, the $1D^{10}$ orbital has an exchange splitting and is expected to follow Hund's rule of filling the majority spin states first. If the V atom is in the center of the cluster, the 3d orbitals of V may not hybridize with the 1P delocalized orbitals due to symmetry. However, in this case, the V atom is on the edge of the cluster, so the 3d orbital has some contribution to the $1P_z$ orbital.

For $^5Ag_8V^+$, the electronic configuration is $1S^2$, $1P^6$, $3d_\alpha^4$ with a spin multiplicity of 5. This indicates that there are eight delocalized electrons in the 1S and 1P orbitals, and the four 3d orbitals are fairly localized. $^4Ag_9V^+$ has the additional electron in $3d_\beta^1$ orbital with a decrease in multiplicity to 4. This cluster now has five electrons in 3d/1D orbitals, so at this point the additional Ag electrons must at least partly hybridize with the V atoms. $^5Ag_{10}V^+$ has the majority $3d_\alpha^5$ shell filled and an electron in the minority shell. From this point onward, the successive electrons fill the minority states, leading to a progressive quenching of the spin magnetic moment as one reaches the size $^1Ag_{14}V^+$. $^3Ag_{12}V^+$ has a cuboctahedral structure with O_h symmetry, and as Figure 5 shows the highest occupied molecular orbitals have distinct degeneracies. The electron count for this cluster is 16 electrons, two less than needed for a shell closing with a configuration of $1S^2$ $1P^6$ $1D^{10}$. However, in the $^3Ag_{12}V^+$ cluster, the 3d shell splits into two subshells, a 3-fold degenerated t_{2g} shell and a 2-fold degenerated e_g shell. They are occupied with six and two electrons, respectively. Thus, a Jahn–Teller distortion due to the partially filled e_g shells is expected. However, this is not what we observe. Instead, the ground state multiplicity of the cluster is raised to a triplet that yields a half-filled (α electrons only) e_g shell as the

dx.doi.org/10.1021/ja412064c | J. Am. Chem. Soc. 2014, 136, 8229–8236

HOMO of this system. This is due to the enhanced binding energy of high symmetry structure with a closed geometric shell trumps that of the electron pairing. $^{1}Ag_{14}V^{+}$ has 18 valence electrons and attains a closed electronic shell with an electronic configuration of $1S^2\ 1P^6\ 1D^{10}$. At this point, the 3d orbitals are delocalized with the hybridization between 3d V orbitals and the 1D delocalized orbitals. Addition of a Ag atom to form $^{2}Ag_{15}V$ results in the occupation of 1F orbitals. When the transition metal atom is in the center of the cluster, the 3d orbitals of V may only hybridize with the 1D nearly free electron orbitals due to symmetry. This means that after $^{4}Ag_{10}V^{+}$ the 3d orbitals and delocalized 1D orbitals hybridize. They maintain some exchange splitting from the 3d orbitals of V. The valence of the V atom evolves toward a value of 5 as n in the Ag_nV^{+} cluster charges from 10 to 14.

The above analysis indicates three prominent clusters with filled shells. First, a $^{4}Ag_5V^{+}$ cluster has a planar structure of Ag atoms and has filled 1S, $1P_x$, and $1P_y$ shells with three electrons in the V 3d states, resulting in an effective magic number of six electrons as found by Janssens et al.[49] Next, $^{4}Ag_7V^{+}$ has filled 1S, 1P shells again with three electrons in the V 3d states. The filled 1S, 1P shells make it a magic cluster with eight electrons derived from the $4s^2$ state of V and $5s^1$ states of Ag atoms. The 3d state of V have atomic configuration and the cluster has an effective valence of 2. Finally a $^{1}Ag_{14}V^{+}$ cluster has an electronic configuration of $1S^2\ 1P^6\ 3d/1D^{10}$ with a valence of 5 for V and is a magic cluster of 18 electrons. As we now show, these shell closures lead to enhanced stability and observable features in the electronic properties. We first consider the energetic stability of clusters. We examined the energy gained in adding a Ag atom to the preceding size

$$\Delta E_{Ag} = -E(Ag_nV^{+}) + E(Ag) + E(Ag_{n-1}V^{+}) \quad (1)$$

where E is the total energy of the indicated species. Figure 6A shows the variation of ΔE_{Ag} as a function of size for the cations and neutral Ag_nV clusters. As the experimental data is available on cations, we primarily focus on these species. Note that there are local maxima for Ag_nV^{+} clusters containing 5, 7, and 14 Ag atoms. In each case, there is an increase in energy gain in forming the cluster from preceding size and a decrease in the energy gain in going to the next size. This is in agreement with the experimental observations that show significant drop in intensity after n values of 5, 7, and 14. In addition to these sizes, there is a local maxima at n = 12. Note that the maxima at $Ag_{12}V^{0/+}$ is shown both by the neutral and cationic species. This maxima corresponds to a geometrical shell closure as binding energies trends are sensitive both to geometric shell closures and electronic shell closures. In addition to removal of a Ag atom, one can also consider stability toward the removal of vanadium. We examined the stability corresponding to a removal of V and V^{+} by calculating ΔE_V and ΔE_V^{+} defined as follows.

$$\Delta E_V = -E(Ag_nV^{+}) + E(V) + E(Ag_n^{+}) \quad (2)$$

$$\Delta E_V^{+} = -E(Ag_nV^{+}) + E(V^{+}) + E(Ag_n) \quad (3)$$

The results are shown in Figure 6B. Note that the removal energy for a V atom (empty circles) shows maxima at n = 6, 8, and 14. The corresponding removal energy for a V^{+} (filled circles), however, shows maxima at n = 5, 7, and 13.

A Bader charge analysis (see Supporting Information Table SI-1), shows that the net charge on the V site is around +1 e^{-},

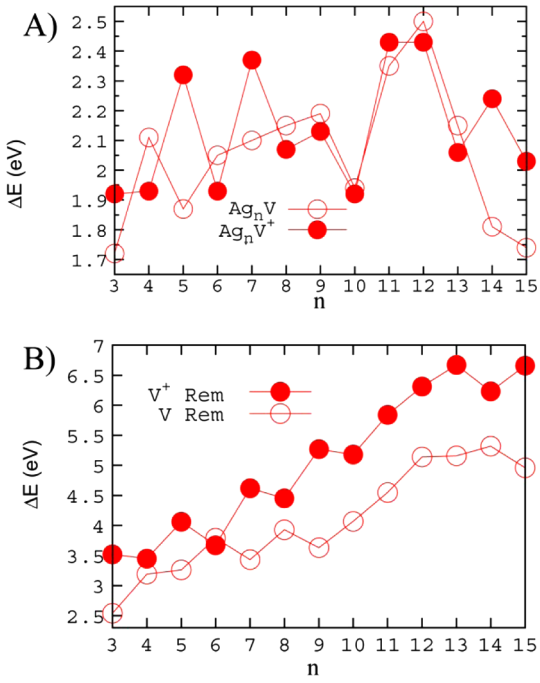

Figure 6. Binding energy (BE; in electronvolts) of (A) one Ag atom to the $Ag_nV^{0/+}$ clusters (eq 1) and the BE of the (B) $V^{0/+}$ to the Ag_nV^{+} clusters (eqs 2 and 3) as a function of the number of Ag atoms ($3 \leq n \leq 15$).

either for neutral or cations of $Ag_nV^{0/+}$. The energy to remove a V atom is, however, lower than that for V^{+} for almost all cases. This indicates that the structural rearrangements upon removal of V/V^{+} play a determining role on the fragmentation energies.

In addition to energetic stability, clusters with filled shells also exhibit chemical stability. One measure of such a stability is the gap between the highest occupied molecular orbital (HOMO) and the lowest unoccupied molecular orbital (LUMO). A large HOMO−LUMO gap is a signature of the chemical stability as the cluster wants to neither donate nor receive charge. Figure 7 shows the HL gap in the neutral and

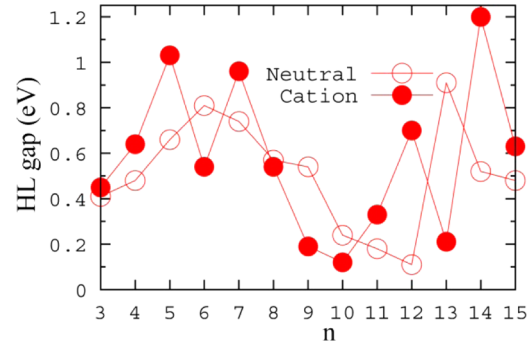

Figure 7. HOMO−LUMO gap (in electronvolts) as a function of the number of Ag atoms for the ground state Ag_nV^{+} clusters ($3 \leq n \leq 15$).

cationic clusters. For the cationic clusters, Figure 7 shows large HOMO−LUMO gaps for Ag_nV^{+} clusters containing 5, 7, and 14 atoms reiterating their stability. There is also a local maximum in the HOMO−LUMO gap for $Ag_{12}V^{+}$, the cuboctahedral closed geometric shell cluster, which is caused by the cluster having its 3d-shell filled in the spin up channel, and an unusually large subshell splitting in the spin down

dx.doi.org/10.1021/ja412064c | J. Am. Chem. Soc. 2014, 136, 8229−8236

channel due to the clusters' highly symmetric structure. For the neutral clusters, the maxima occur at 6 and 13 because the cluster has an extra electron. Although one would also expect a large gap from $^4Ag_4V$, the HOMO is spin-down, whereas the LUMO is spin-up. The gaps within the spin manifolds correspond to 0.73 and 1.28 eV for the α and β channels, and would result in a local maximum in the HOMO−LUMO gaps in the Ag_nV series.

The so-far discussed data suggests that the trends exhibited by cationic Ag_nV^+ clusters as a function of size should be similar to those of neutral $Ag_{n-1}V$ clusters. To this end, we calculated the vertical (VIP) and adiabatic ionization potentials (AIP) of the neutral species. Figure 8 shows the calculated values as a

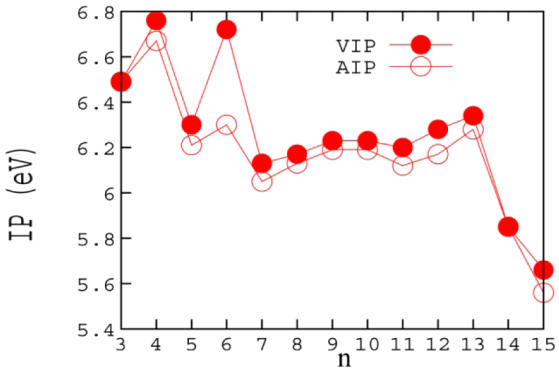

Figure 8. Adiabatic ionization potential (AIP) and vertical ionization potential (VIP) as a function of the number of Ag atoms.

function of size. Note that clusters with 5, 7, 14, and 15 atoms have lower ionization potential than the neighboring sizes. The lower ionization along with the electronic stability accounts for the drop in intensity after 5, 7, and 14 silver atoms.

Figure 8 also brings out an interesting feature, namely, that the trends exhibited by Ag_nV^+ clusters as a function of size are replicated by $Ag_{n-1}V$ clusters. In this respect, it supports the enhanced stability of cationic species at n = 4, 6, and 13.

The change in valence results in a change in the number of unpaired electrons, and hence, we now consider the variation in the spin multiplicity as a function of size. Figure 9 shows the variation in the spin multiplicity of the neutral and cationic clusters. A V atom has a spin multiplicity of 4. For the cationic species, the multiplicity initially alternates between 5 and 4

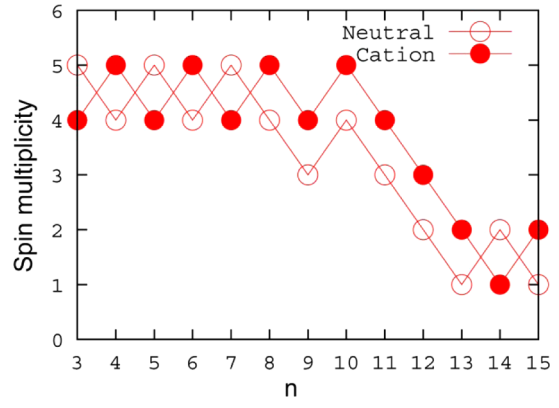

Figure 9. Variation of the spin multiplicity of the ground state Ag_nV^+ clusters (unfilled red spheres) and Ag_nV clusters (filled blue spheres) as a function of the number or Ag atoms ($3 \leq n \leq 15$).

starting from $^5Ag_4V^+$, but from $^5Ag_{10}V^+$, it progressively decreases to singlet for $^1Ag_{14}V^+$. For the neutral clusters, the spin multiplicity starts to decrease at $^4Ag_{10}V$ and the magnetic moment is completely quenched for $^1Ag_{13}V$. We note that in all cases except for $^3Ag_9V$ and $^5Ag_{10}V^+$, the magnetic moment is the same for clusters with the same number of valence electrons. At sizes larger than n = 13, for both cations and neutrals, there is an oscillation between singlet and doublet. The progressive decrease in multiplicity at large sizes is consistent with the valence 5 where the d states get progressively filled as discussed earlier.

CONCLUSIONS

To summarize, the present studies confirm that the V atoms in $Ag_nV^{0/+}$ clusters undergo a transition in valence with size and that the valence change is correlated with the symmetry of the superatomic orbitals. The present work reveals that as the size increases, the 3d states of V hybridize with the superatomic D states, and the symmetry constraint is the microscopic origin of this transition. The stability of clusters changes with shell filling and follows a fairly simple scheme depending on whether the cluster is approximately planar or approximately spherical. The first shell closure occurs at Ag_5V^+ where the planar configuration of Ag atoms leads to a filling of 1S, $1P_x$, and $1P_y$ states with the remaining 3 electrons in V 3d states as in an atom. At larger sizes, the structure of the Ag atoms makes a transition to three-dimensional shape where a second stable cluster Ag_7V^+ is observed with filled 1S and 1P shells. Starting with $Ag_{10}V^{0,+}$, however, the multiplicity continuously decreases as the total valence electron count approaches 18, at which point the 1D state is completely filled, the magnetic moment is quenched, and the spin multiplicity alternates between 1 and 2 depending on the even or odd electron count at larger sizes. In addition to electronic effects, the clusters exhibit stability features that can be associated with geometrical shells. It will be nice to examine if other silver clusters doped by transition metal atoms also exhibit similar features.

ASSOCIATED CONTENT

Supporting Information

Supporting Information includes the calculated atomic states of V and V^+, Cartesian coordinates of the optimized structures, Bader charges of the V atoms as a function of cluster size, lowest energy normal modes, and the calculated Mulliken valence of vanadium in the clusters. This material is available free of charge via the Internet at http://pubs.acs.org.

AUTHOR INFORMATION

Corresponding Author

snkhanna@vcu.edu; pcalamin@cinvestav.mx; akoster@cinvestav.mx

Notes

The authors declare no competing financial interest.

ACKNOWLEDGMENTS

V.M.M., A.C.R., and S.N.K. gratefully acknowledge support from U. S. Department of Energy (DOE) through grant DE-FG02-11ER16213. P.C. and A.M.K. acknowledge financial support from CONACYT (Grants CB-130726 and CB-179409) and computing facilities from the WestGrid of Compute Canada. V.C. and P.S. acknowledge use of the cluster computing facility at HRI.

REFERENCES

(1) Knight, W. D.; Clemenger, K.; de Heer, W. A.; Saunders, W. A.; Chou, M. Y.; Cohen, M. L. *Phys. Rev. Lett.* **1984**, *52*, 2141−2143.
(2) Brack, M. *Rev. Mod. Phys.* **1993**, *65*, 677−732.
(3) Clemenger, K. *Phys. Rev. B: Condens. Matter Mater. Phys.* **1985**, *32*, 1359−1362.
(4) Li, X.; Wu, H.; Wang, X.-B.; Wang, L.-S. *Phys. Rev. Lett.* **1998**, *81*, 1909−1912.
(5) Martin, T. P.; Bergmann, T.; Göhlich, H.; Lange, T. *Chem. Phys. Lett.* **1990**, *172*, 209−213.
(6) Wrigge, G.; Hoffmann, M. A.; Issendorff, B. v. *Phys. Rev. A: At., Mol., Opt. Phys.* **2002**, *65*, 063201.
(7) Khanna, S. N.; Jena, P. *Phys. Rev. B: Condens. Matter Mater. Phys.* **1995**, *51*, 13705−13716.
(8) Castleman, A. W.; Khanna, S. N. *J. Phys. Chem. C* **2009**, *113*, 2664−2675.
(9) Janssens, E.; Neukermans, S.; Lievens, P. *Curr. Opin. Solid State Mater. Sci.* **2004**, *8*, 185−193.
(10) Bergeron, D. E.; Castleman, A. W.; Morisato, T.; Khanna, S. N. *Science* **2004**, *304*, 84−87.
(11) Reber, A. C.; Khanna, S. N.; Roach, P. J.; Woodward, W. H.; Castleman, A. W. *J. Am. Chem. Soc.* **2007**, *129*, 16098−16101.
(12) Knight, W. D.; Clemenger, K.; de Heer, W. A.; Saunders, W. A. *Phys. Rev. B: Condens. Matter Mater. Phys.* **1985**, *31*, 2539−2540.
(13) Ganteför, G.; Gausa, M.; Meiwes-Broer, K.-H.; Lutz, H. O. *J. Chem. Soc., Faraday Trans.* **1990**, *86*, 2483−2488.
(14) Handschuh, H.; Cha, C.-Y.; Bechthold, P. S.; Ganteför, G.; Eberhardt, W. *J. Chem. Phys.* **1995**, *102*, 6406−6422.
(15) Leuchtner, R. E.; Harms, A. C.; Castleman, A. W. *J. Chem. Phys.* **1989**, *91*, 2753.
(16) Socaciu, L. D.; Hagen, J.; Heiz, U.; Bernhardt, T. M.; Leisner, T.; Wöste, L. *Chem. Phys. Lett.* **2001**, *340*, 282−288.
(17) Bernhardt, T. M. *Int. J. Mass Spectrom.* **2005**, *243*, 1−29.
(18) Schmidt, M.; Masson, A.; Bréchignac, C. *Phys. Rev. Lett.* **2003**, *91*, 243401.
(19) Socaciu, L. D.; Hagen, J.; Le Roux, J.; Popolan, D.; Bernhardt, T. M.; Wöste, L.; Vajda, Š. *J. Chem. Phys.* **2004**, *120*, 2078−2081.
(20) Hagen, J.; Socaciu, L. D.; Le Roux, J.; Popolan, D.; Bernhardt, T. M.; Wöste, L.; Mitrić, R.; Noack, H.; Bonačić-Koutecký, V. *J. Am. Chem. Soc.* **2004**, *126*, 3442−3443.
(21) Schmidt, M.; Masson, A.; Bréchignac, C. *J. Chem. Phys.* **2005**, *122*, 134712−134712−4.
(22) Bernhardt, T. M.; Hagen, J.; Lang, S. M.; Popolan, D. M.; Socaciu-Siebert, L. D.; Wöste, L. *J. Phys. Chem. A* **2009**, *113*, 2724−2733.
(23) Bergeron, D. E.; Roach, P. J.; Castleman, A. W.; Jones, N. O.; Khanna, S. N. *Science* **2005**, *307*, 231−235.
(24) Reveles, J. U.; Khanna, S. N.; Roach, P. J.; Castleman, A. W. *Proc. Natl. Acad. Sci. U. S. A.* **2006**, *103*, 18405−18410.
(25) Reber, A. C.; Khanna, S. N.; Castleman, A. W. *J. Am. Chem. Soc.* **2007**, *129*, 10189−10194.
(26) Walter, M.; Akola, J.; Lopez-Acevedo, O.; Jadzinsky, P. D.; Calero, G.; Ackerson, C. J.; Whetten, R. L.; Grönbeck, H.; Häkkinen, H. *Proc. Natl. Acad. Sci. U. S. A.* **2008**, *105*, 9157−9162.
(27) Reveles, J. U.; Clayborne, P. A.; Reber, A. C.; Khanna, S. N.; Pradhan, K.; Sen, P.; Pederson, M. R. *Nat. Chem.* **2009**, *1*, 310−315.
(28) Medel, V. M.; Reveles, J. U.; Khanna, S. N.; Chauhan, V.; Sen, P.; Castleman, A. W. *Proc. Natl. Acad. Sci. U. S. A.* **2011**, *108*, 10062−10066.
(29) Abreu, M. B.; Powell, C.; Reber, A. C.; Khanna, S. N. *J. Am. Chem. Soc.* **2012**, *134*, 20507−20512.
(30) Zhang, X.; Wang, Y.; Wang, H.; Lim, A.; Gantefoer, G.; Bowen, K. H.; Reveles, J. U.; Khanna, S. N. *J. Am. Chem. Soc.* **2013**, *135*, 4856−4861.
(31) Fernández, E. M.; Soler, J. M.; Garzón, I. L.; Balbás, L. C. *Phys. Rev. B: Condens. Matter Mater. Phys.* **2004**, *70*, 165403.
(32) Tian, D.; Zhang, H.; Zhao, J. *Solid State Commun.* **2007**, *144*, 174−179.
(33) Fournier, R. *J. Chem. Phys.* **2001**, *115*, 2165−2177.
(34) Alamanova, D.; Grigoryan, V. G.; Springborg, M. *J. Phys. Chem. C* **2007**, *111*, 12577−12587.
(35) Yang, X.; Cai, W.; Shao, X. *J. Phys. Chem. A* **2007**, *111*, 5048−5056.
(36) Yang, M.; Jackson, K. A.; Jellinek, J. *J. Chem. Phys.* **2006**, *125*, 144308.
(37) Baishya, K.; Idrobo, J. C.; Öğüt, S.; Yang, M.; Jackson, K.; Jellinek, J. *Phys. Rev. B: Condens. Matter Mater. Phys.* **2008**, *78*, 075439.
(38) Gamboa, G. U.; Reber, A. C.; Khanna, S. N. *New J. Chem.* **2013**, *37*, 3928−3935.
(39) Luo, Z.; Gamboa, G. U.; Smith, J. C.; Reber, A. C.; Reveles, J. U.; Khanna, S. N.; Castleman, A. W. *J. Am. Chem. Soc.* **2012**, *134*, 18973−18978.
(40) Walter, M.; Häkkinen, H. *Phys. Chem. Chem. Phys.* **2006**, *8*, 5407−5411.
(41) Wang, L.-M.; Pal, R.; Huang, W.; Zeng, X. C.; Wang, L.-S. *J. Chem. Phys.* **2009**, *130*, 051101.
(42) Roach, P. J.; Woodward, W. H.; Reber, A. C.; Khanna, S. N.; Castleman, A. W. *Phys. Rev. B: Condens. Matter Mater. Phys.* **2010**, *81*, 195404.
(43) Luo, Z.; Grover, C. J.; Reber, A. C.; Khanna, S. N.; Castleman, A. W. *J. Am. Chem. Soc.* **2013**, *135*, 4307−4313.
(44) Gruner, G.; Zawadowski, A. *Rep. Prog. Phys.* **1974**, *37*, 1497.
(45) Van der Marel, D.; Sawatzky, G. A.; Hillebrecht, F. U. *Phys. Rev. Lett.* **1984**, *53*, 206−209.
(46) Friedel, J. *Nuovo Cimento* **1958**, *7*, 287−311.
(47) Kondo, J. *Prog. Theor. Phys.* **1964**, *32*, 37−49.
(48) Neukermans, S.; Janssens, E.; Tanaka, H.; Silverans, R. E.; Lievens, P. *Phys. Rev. Lett.* **2003**, *90*, 033401.
(49) Janssens, E.; Tanaka, H.; Neukermans, S.; Silverans, R. E.; Lievens, P. *New J. Phys.* **2003**, *5*, 46.
(50) Janssens, E.; Tanaka, H.; Neukermans, S.; Silverans, R. E.; Lievens, P. *Phys. Rev. B: Condens. Matter Mater. Phys.* **2004**, *69*, 085402.
(51) Nhat, P. V.; Nguyen, M. T. *Phys. Chem. Chem. Phys.* **2011**, *13*, 16254.
(52) Janssens, E.; Neukermans, S.; Nguyen, H. M. T.; Nguyen, M. T.; Lievens, P. *Phys. Rev. Lett.* **2005**, *94*, 113401.
(53) Janssens, E.; Neukermans, S.; Wang, X.; Veldeman, N.; Silverans, R. E.; Lievens, P. *Eur. Phys. J. D: At., Mol. Opt. Phys.* **2005**, *34*, 23−27.
(54) Martin, T. P.; Bergmann, T.; Göhlich, H.; Lange, T. *Chem. Phys. Lett.* **1991**, *176*, 343−347.
(55) Martin, T. P.; Näher, U.; Bergmann, T.; Göhlich, H.; Lange, T. *Chem. Phys. Lett.* **1991**, *183*, 119−124.
(56) Perdew, J. P.; Yue, W. *Phys. Rev. B: Condens. Matter Mater. Phys.* **1986**, *33*, 8800−8802.
(57) Perdew, J. P. *Phys. Rev. B: Condens. Matter Mater. Phys.* **1986**, *33*, 8822−8824.
(58) Köster, A. M.; Calaminici, P.; Casida, M. E.; Dominguez, V. D.; Flores-Moreno, R.; Gamboa, G. U.; Goursot, A.; Heine, T.; Ipatov, A.; Janetzko, F. *deMon2k Program*; The deMon Developers: Cinvestav, Mexico City, 2011
(59) Calaminici, P.; Janetzko, F.; Köster, A. M.; Mejia-Olvera, R.; Zuniga-Gutierrez, B. *J. Chem. Phys.* **2007**, *126*, 044108−044108−10.
(60) Dunlap, B. I.; Connolly, J. W. D.; Sabin, J. R. *J. Chem. Phys.* **1979**, *71*, 3396−3402.
(61) Reveles, J. U.; Khanna, S. N.; Köster, A. M. *J. Mol. Struct.: THEOCHEM* **2006**, *762*, 171−178.
(62) Calaminici, P.; Köster, A. M., Jr.; C, T.; Roy, P.-N.; Russo, N.; Salahub, D. R. *J. Chem. Phys.* **2001**, *114*, 4036−4044.
(63) Andrae, D.; Häußermann, U.; Dolg, M.; Stoll, H.; Preuß, H. *Theor. Chim. Acta* **1990**, *77*, 123−141.
(64) Bader, R. F. W. *Chem. Rev.* **1991**, *91*, 893−928.
(65) Rodríguez, J. I.; Köster, A. M.; Ayers, P. W.; Santos-Valle, A.; Vela, A.; Merino, G. *J. Comput. Chem.* **2009**, *30*, 1082−1092.
(66) Martins, J. L.; Buttet, J.; Car, R. *Phys. Rev. B: Condens. Matter Mater. Phys.* **1985**, *31*, 1804−1816.

(67) Rao, B. K.; Khanna, S. N.; Jena, P. *Phys. Rev. B: Condens. Matter Mater. Phys.* **1987**, *36*, 953−960.
(68) Jug, K.; Zimmermann, B.; Calaminici, P.; Köster, A. M. *J. Chem. Phys.* **2002**, *116*, 4497−4507.
(69) Jug, K.; Zimmermann, B.; Köster, A. M. *Int. J. Quantum Chem.* **2002**, *90*, 594−602.